Alex Chansky
Remote Sensing Final Project Report, May 2020

Damage Detection and Land Classification for the 2001 Nisqually Earthquake

Introduction and Goals

This project aimed to detect change after the 2001 Nisqually earthquake with the secondary goal of classifying land use. Primary goals included determining the kinds of change which can be seen at 30-meter resolution and how much change detection improves by sharpening an image with the panchromatic band. Secondary goals included determining the best method for classifying urban areas, as well as determining the utility of masks and textural filters for improving classifications.

The 6.8 moment magnitude earthquake resulted in severe damage in several urban areas, with some of the larger damages resulting in cracks over 80 meters long. In theory, these damages could be noticed even with low levels of resolution. By taking images from the Landsat satellites before and after the event and making appropriate corrections, differencing the images should reveal changes where damages occurred. The project also began with the secondary goal of classifying land use. This could help identify the types of urban areas where damages occurred. This is especially important for estimating damages due to liquefaction, which occurred in the Nisqually earthquake but can be difficult to study because it does not occur often. By linking known dollar values of liquefaction damage to these different urban areal classifications, such as roads, a dollar value of damage can be assigned per pixel of infrastructure. If the same amount of liquefaction risk is expected in a different area for future events, multiplying the number of pixels of infrastructure by the liquefaction damage per pixel found in this project will provide an estimate for liquefaction damage of that infrastructure type.

The 2001 Nisqually earthquake caused damage primarily in two urban areas in Washington state: Seattle and Olympia. Many of these damages were due to a secondary hazard in earthquakes known as liquefaction and can be observed on a large scale (**figures 1, 2, 3,** and **4**) These figures are all taken from the 2001 Geer Association report[1]. While other damages should also be visible from imagery, damages due to the liquefaction have geographic locations and dollar values of damage associated with them which will be useful for future work if the project is successful in detecting change at damage locations.


Figures 1 and **2**: Road and walkway damages due to liquefaction in the 2001 Nisqually earthquake at the Deschutes Parkway.


Figures 3 and **4**: Road damages due to liquefaction in a residential neighborhood in the 2001 Nisqually earthquake near Sunset Lake, Olympia. *Images sourced from geerassociation.org.*

Workflow

For this project to be successful, it was important first to focus on best strategies for change detection. Image differencing was to be conducted on the images at 30-meter resolution, followed by Gram-Schmidt sharpening using the panchromatic band, and image differencing of the higher resolution images (**figure 5**).

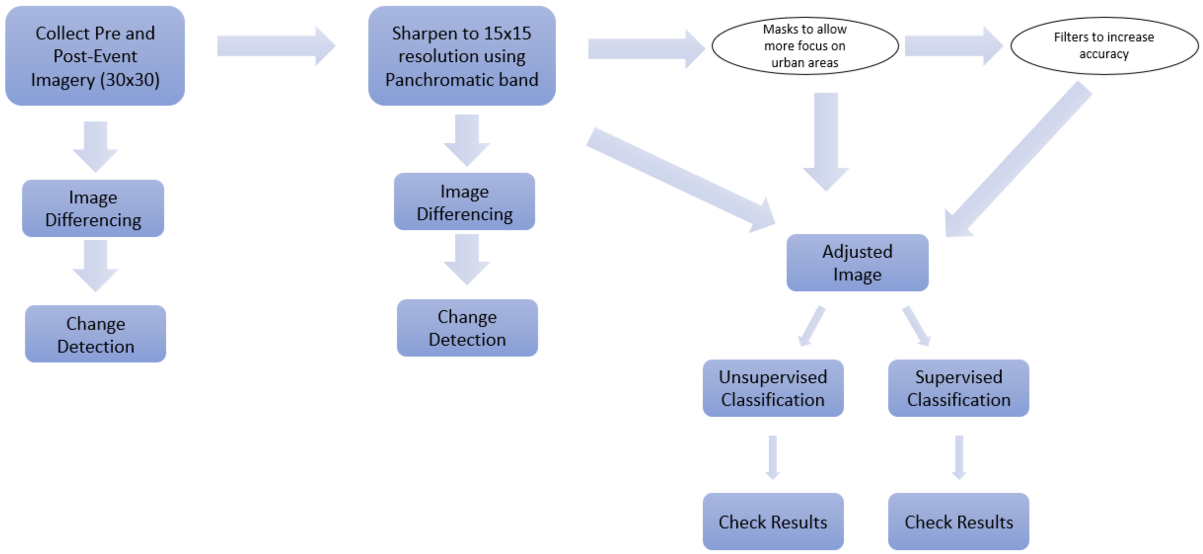

Figure 5: Workflow of methodology for the project.

Next, different classifications would be addressed using the sharpened version of either the pre- or post-event imagery. This would be determined based on a visual assessment of cloud and vegetation cover to determine which image revealed more infrastructure. After trying several methods to determine the best method for the data, binary masks would be applied to either eliminate water bodies or eliminate everything except urban areas, followed by the same classification methods applied to the original image. This would be followed by applying textural filters to the masked images before applying the same classification methods. Although somewhat repetitive, iterating through all the combinations of masks, filters, and classification methods will determine the most accurate classification scheme for the image.

Data Collection

All images for this project were gathered from the USGS Earth Explorer website[2]. Original images for the project were downloaded from the "Analysis Ready Data" section, which includes images from Landsat satellites with some corrections and edits. After using these images to complete image differencing, it was discovered that the analysis ready data did not contain panchromatic bands. To use panchromatic bands for sharpening and improved image analysis, level 1 images were needed. The images had to be selected carefully to ensure they contained the area of interest with few clouds. Part of Seattle and its surrounding urban sprawl is cut off by the pre-event image, while Olympia is successfully contained within both images, which led to a focus on Olympia for the remainder of the project (**figures 6** and **7**).

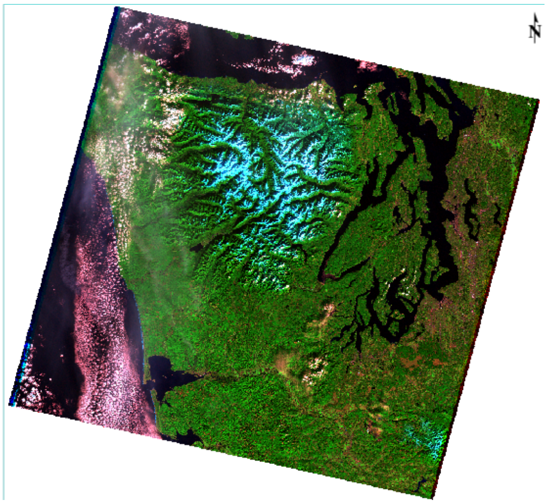

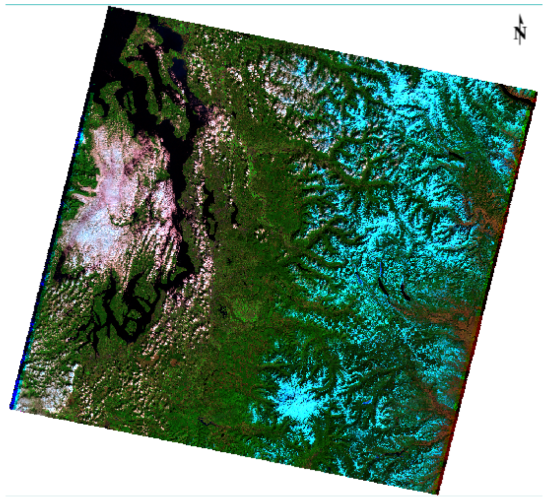

Figures 6 and **7**: Pre-event (left) and post-event (right) imagery used in this project.

Processing and Analysis

Based on a visual interpretation of all six bands in the region of interest where damage was expected, it would have been very difficult to detect any changes using 30-meter resolution. To ensure enough time was spent on the rest of the project to obtain reasonable results, the image differencing on 30-meter resolution was skipped and the project shifted focus to analyzing image differences at 15-meter resolution. This step was completed using Gram-Schmidt pan sharpening method, which creates a low-resolution panchromatic band with weighted averages of the original multispectral bands. Then, the bands are decorrelated with the Gram-Schmidt algorithm and the low-resolution panchromatic band is replaced with its corresponding high-resolution band, and bands are back transformed into high-resolution[3]. **Figures 8** and **9** show the sharpened pre- and post-event imagery after Gram-Schmidt panchromatic sharpening.

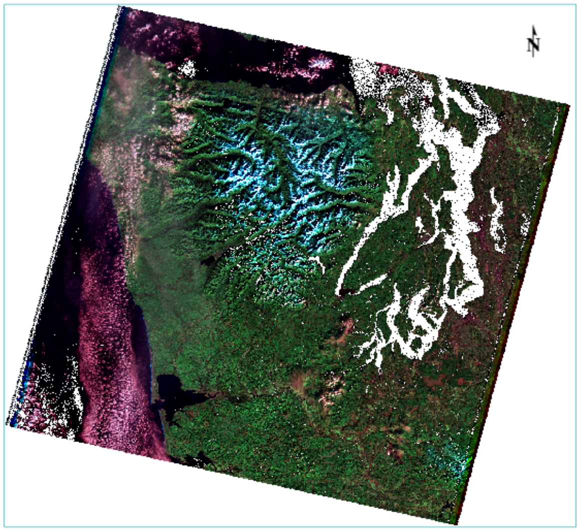

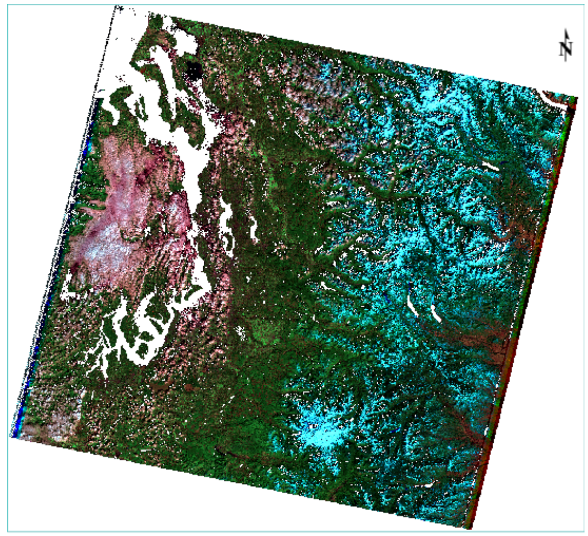

Figures 8 and **9**: Pre- (left) and post-event (right) images after applying Gram-Schmidt algorithm.

In the next step, the images were cut down to the region of interest (Olympia and its surrounding urban sprawl) and displayed in RGB with bands 7, 4, and 2 to observe a variety of reflectance (**figure 8**). Several issues appear in these images which could lead to high difference values without any correlation to areas impacted by the earthquake. Firstly, there is significantly more vegetation in the post-event imagery. The post-event image was taken in mid-March instead of early February, which in Washington is enough time for significant vegetation growth. Secondly, the pre-event image is clear of clouds while the post-event image has enough clouds to be potentially problematic. Most of the clouds occur outside of the urban area, so a focus on only urban areas should reduce this issue. Lastly, in the pre-event image, some water bodies have some values while the post-event images do not, which will result in varying values across a water body when image differencing is completed.

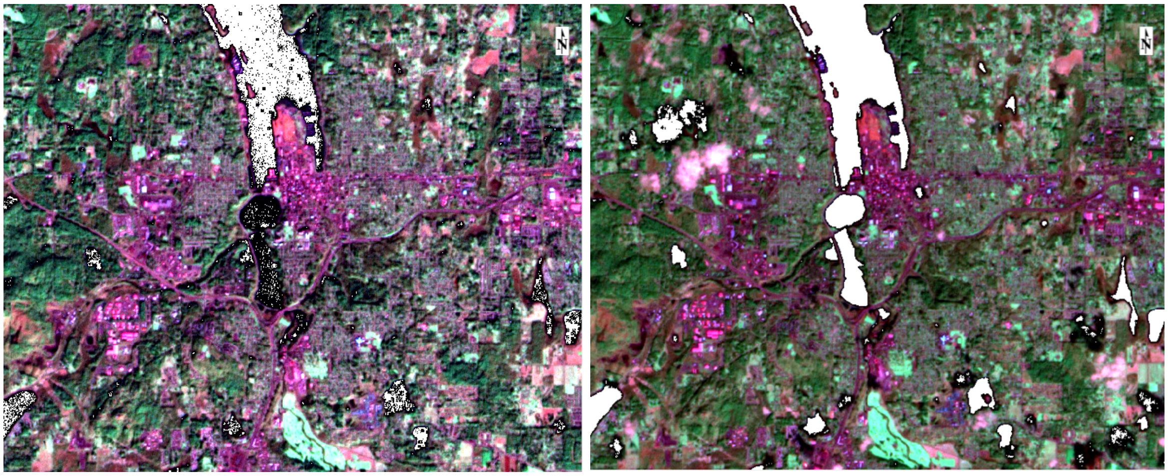

Figures 10 and **11**: Area of interest after panchromatic sharpening displayed in RGB with bands 7, 4, and 2.

To eliminate issues due to vegetation, clouds, and water bodies, an index was calculated to isolate urban areas for observation. Using the normalized difference built-up index (NDBI), values were computed for every pixel in the pre-event imagery by dividing the difference of shortwave infrared and near-infrared values by the summation of the same two bands[4]. This index helps to identify built-up urban areas. The pre-event imagery was used because it is clearer of clouds and vegetation than the post-event image. By visually assigning a threshold value of 0.02, a binary mask was produced where every pixel with an NDBI value above 0.02 contained a "built-up" area (**figure 12**). The image bands were differenced and stacked in **figure 13**, then the built-up binary mask was applied to observe only the built-up areas (**figure 14**).

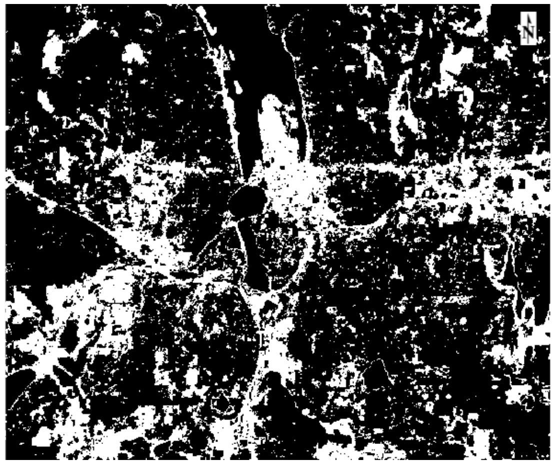

Figure 12: Binary mask with built-up areas having NDBI greater than 0.02 and marked in white.

Figure 13: Stacked image difference with bands 7, 4, and 2 displayed in RGB.

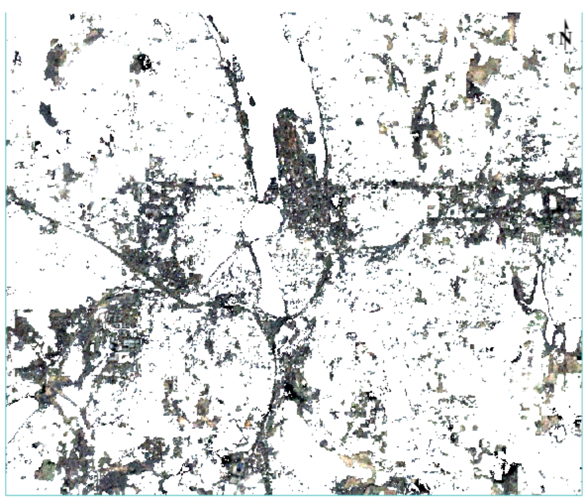

Figure 14: Stacked image difference after NDBI mask was applied.

An analysis of the image difference reveals that the change detection was less successful than intended. For example, a section of the band 4 image differencing results after the NDBI mask was applied is displayed in **figure 15**, with dark red areas indicating high amounts of negative change in band four. At first glance, expected areas of damage highlighted by red boxes are distinguished well by red negative change due to image differencing. However, after zooming out in **figure 16**, we see that there are many other bright red zones across our area of interest where damage was not expected, so this method may not be very reliable. Similar inconsistencies in change detection were observed across all bands.

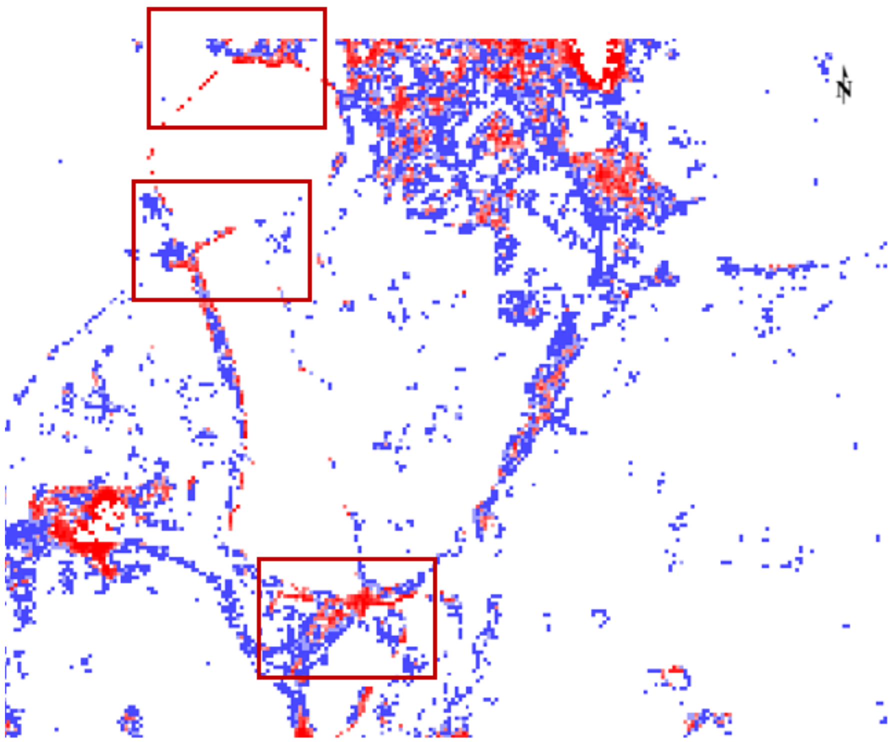

Figure 15: Band 4 difference with areas of strong negative change in dark red and areas of strong positive change in dark blue.

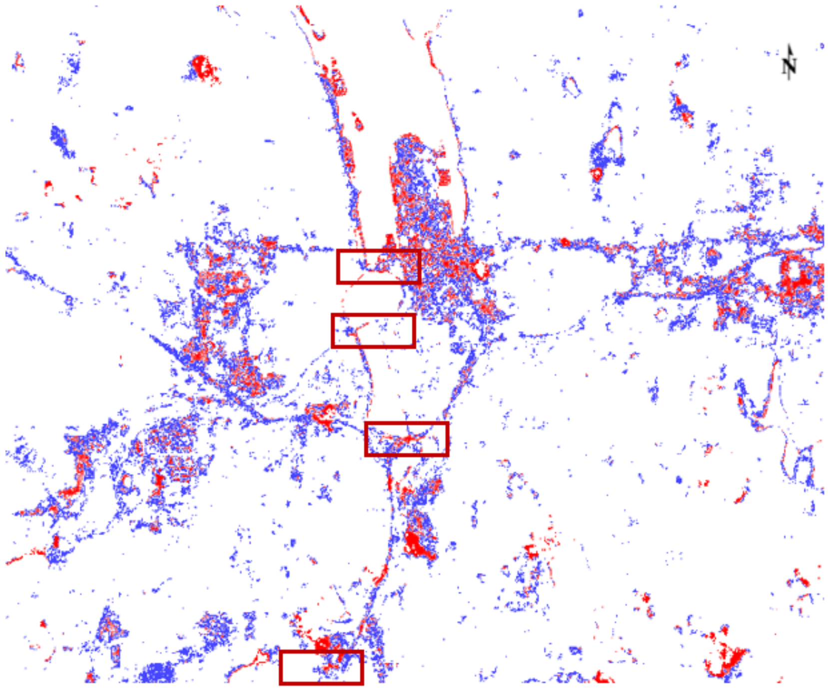

Figure 16: Band 4 difference with areas of strong negative change in dark red and areas of strong positive change in dark blue.

Next, land use classification attempts were made using several supervised and unsupervised classification methods on the original imagery. Occurrence and co-occurrence textural filters were applied to the image to preserve boundary layers of features in the image. This is oftentimes used as a tool to help increase classification accuracy. Occurrence filters produce five textural components using a 3x3 kernel for each band, such as mean and variance. This produces a total of 30 components across six bands for each pixel (**figure 17**). Co-occurrence filters produce eight textural components for each band, producing a total of 48 components across six bands for every pixel (**figure 18).**

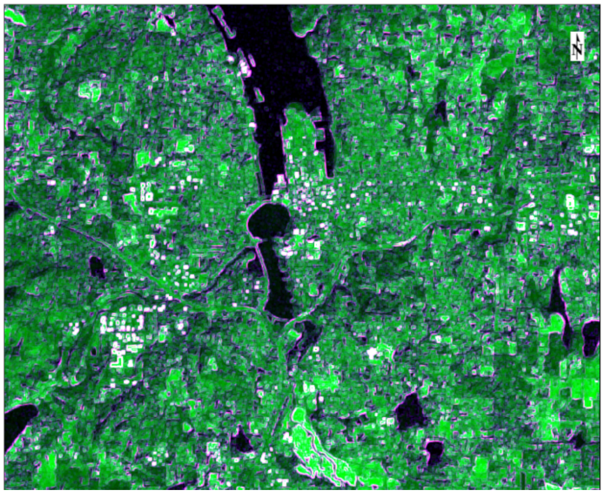 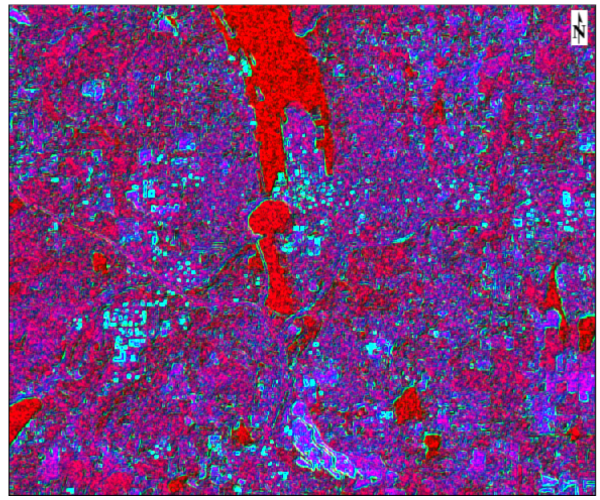

Figures 17 and **18:** Occurrence filter (left) and co-occurrence filter (right) applied to the pre-event imagery.

If a mask was applied before the textural filters were applied, textures surrounding water bodies would be dominated by the lack of data nearby. It would then be very difficult for the classification methods to discern differences between vegetation, roads, or buildings surrounding the water bodies, which was very important for this project. In the remaining steps of the project, wherever a textural filter is combined with a classification attempt, the textural filter is applied before any masking is done.

The pre-event image was used for classification due to its lack of clouds and vegetation, meaning urban areas could be more easily analyzed. During the first classification attempt, a k-means classification was run on the image after applying the built-up mask and an occurrence filter was applied, seen in **figure 19**. In k-means clustering, classes are determined by the user, and centroids for each class are placed randomly in a scatterplot with m dimensions, where m represents the number of components used for differentiation. When using k-means classification on the multispectral bands, m was representing the six bands. However, when using k-means for the image where textural filters were applied, m was 30 and 48 for the 30 components of the occurrence filter and 48 components of the co-occurrence filter, respectively. The class for each data point is determined by its closest centroid, new centroids are computed for each class, and this process is repeated iteratively[5].

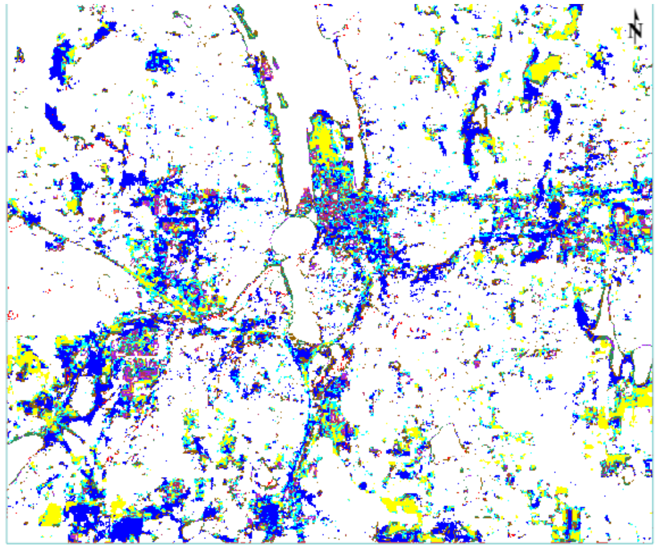

Figure 19: K-means clustering conducted on the results of the occurrence filter.

As seen in **figure 20**, a visual interpretation with ground-truthing after zooming in was used to identify the classes used in k-means classification. However, many pixels in this scene are misclassified so different methods were applied.

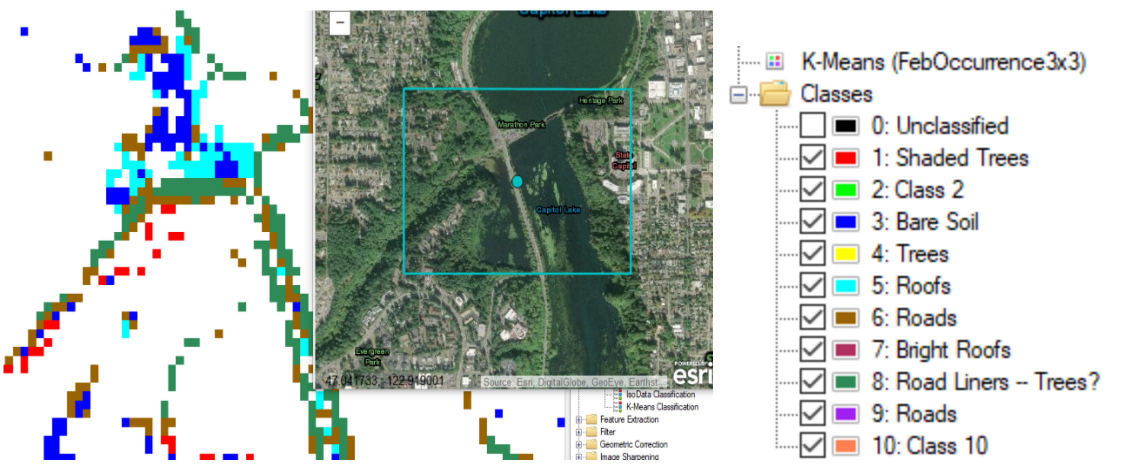

Figure 20: Ground truthing of occurrence k-means classification results.

Next, regions of interest in nine classes were identified and a supervised maximum likelihood classification was applied to the occurrence results. Maximum likelihood classification is a supervised method which requires regions of interest as an input to estimate probability parameters of each class. Each data point will fall into whichever class which it has the highest likelihood of falling into. If a probability threshold is set, then points which have a probability less than the probability threshold will remain unclassified.

This led to more accurate classifications but fewer classifications overall. Even after applying the built-up mask and lowering the threshold classifying probability to 10%, the vast majority pixels remain unclassified (**figure 21**), so more methods were attempted.

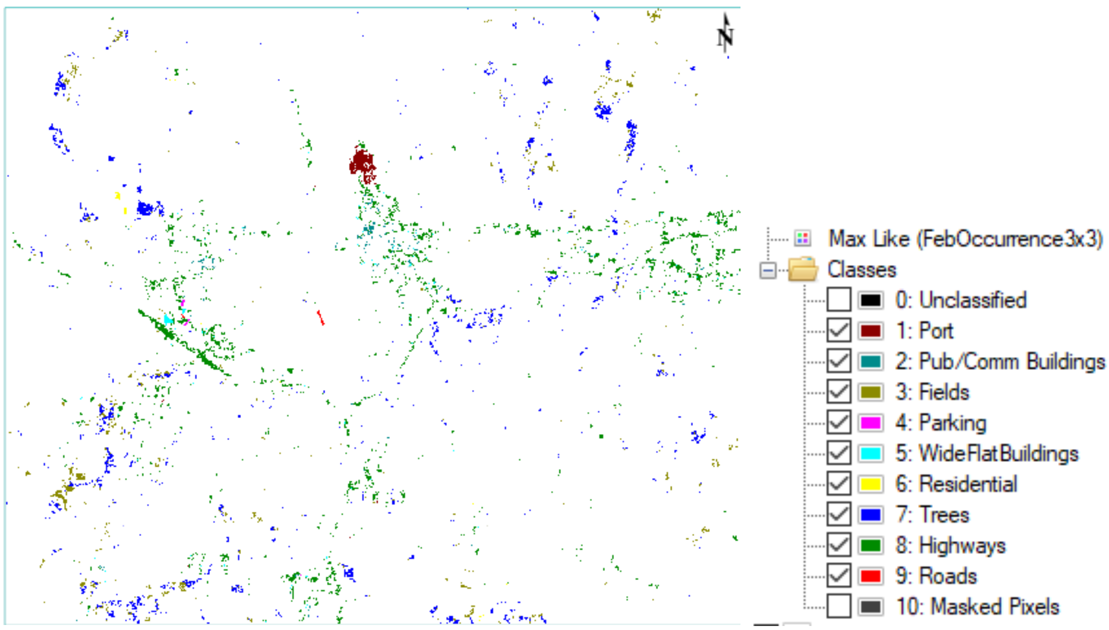

Figure 21: Maximum likelihood results of occurrence filter with 10 classes and threshold probability of 10%.

The supervised parallelepiped method applied to the co-occurrence filter combined with a mask to eliminate water bodies is shown in **figure 22**. While this produced some good classification of urban areas, it did not produce good definition of streets, buildings, residences, and other specificities of urban areas. It also did not identify vegetated areas very well.

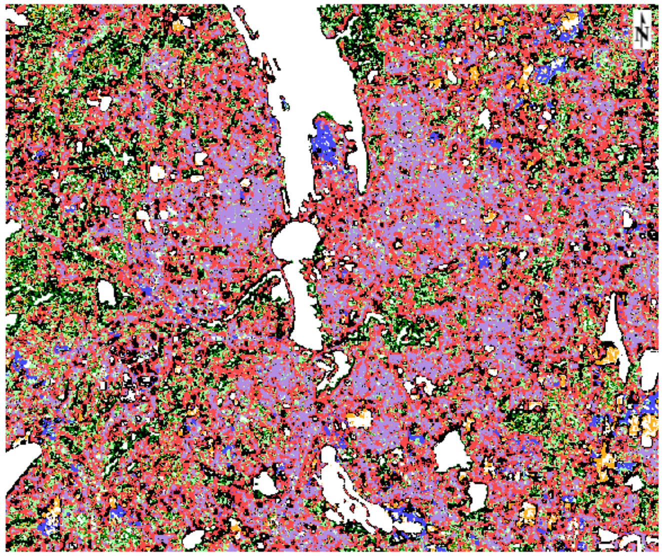

Figure 22: Parallelepiped method applied to results of co-occurrence filter and a water body mask.

In unsupervised classification attempts for the co-occurrence results, it was found that the k-means method worked well to differentiate urban, vegetated, and water regions when only a few classes are specified (**figure 23**). However, the ISODATA method struggled to produce meaningful results. Based on **figure 24** which uses co-occurrence ISODATA results for 10 classes, vegetation and urban areas are often misclassified and even water bodies are split into two different classes.

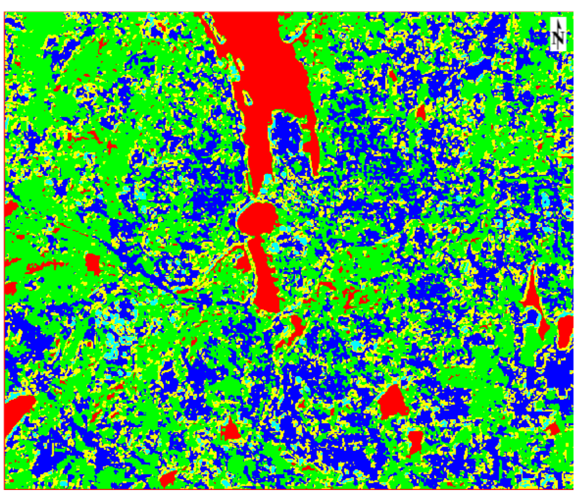

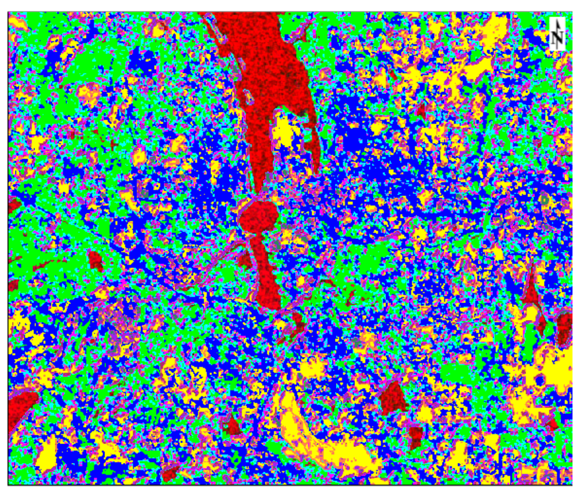

Figures 23 and **24**: K-means (left, 5 classes) and ISODATA (right, 10 classes) applied to co-occurrence filter results.

Some of the best results of the project were obtained from maximum likelihood classification without a probability threshold on the six multispectral bands of the original image rather than its textural filter results. In **figure 25**, nine classes can be verified in many areas by ground-truthing.

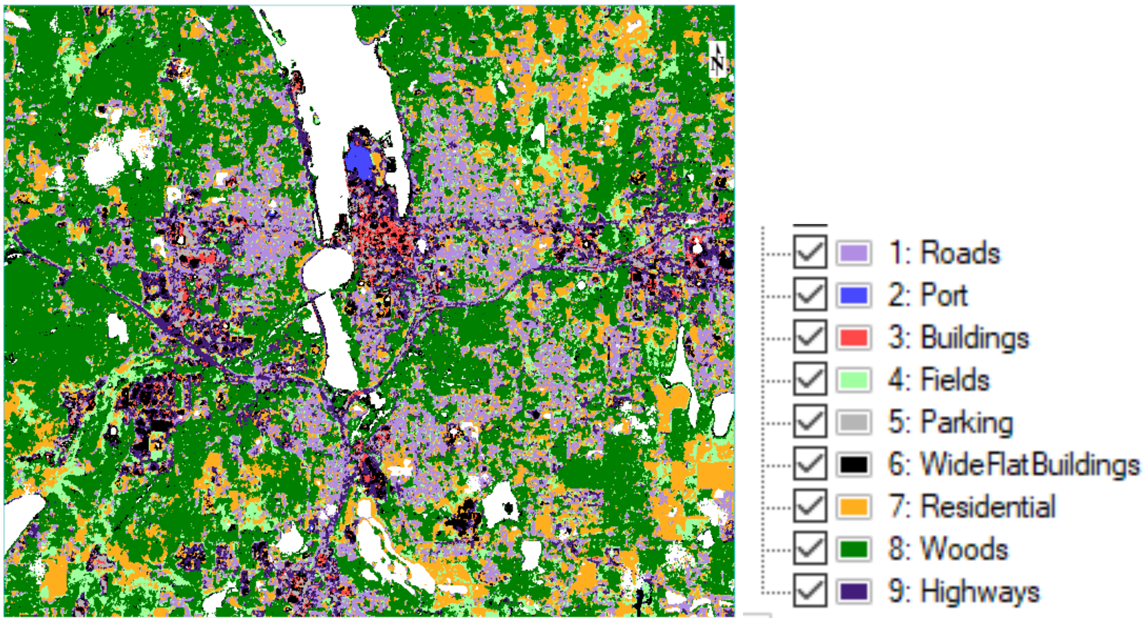

Figure 25: Maximum likelihood classification on six sharpened multispectral bands without a probability threshold, water body mask applied afterwards.

Discussion and Results

For change detection, it can be easily concluded that Gram-Schmidt sharpening using the panchromatic band resulted in images that were much clearer and allowed for change detection of some value to occur. However, the process of simple image differencing failed to yield any results of importance for change detection.

As the best results were obtained by a classification of the original multispectral bands, it can be concluded that the occurrence and co-occurrence filters do not help classification in this data set. Furthermore, as the best classification results were found using a supervised classification system, as long as training data exists, efforts can be focused on improving supervised classification instead of trying unsupervised classification again for identifying land use types. Additional training data will help improve the supervised classification, as well as provide data to check its usefulness with a confusion matrix.

The purpose of the NDBI index in this project was to eliminate non-urban areas so the change detection and classification methods could more easily focus on differentiating values in urban areas. By setting a threshold, pixel values above the threshold could be labeled as urban areas and pixels with values below the threshold could be eliminated with a binary mask. However, after applying this index it was found that many of the urban areas had values below non-urban areas. If a threshold was set on the lower end of acceptable, many urban areas would be eliminated after the mask was applied, but if the threshold was set too high, many vegetative areas would not be eliminated. This means that the index could not be helpful in fully eliminating non-urban areas while retaining urban regions. The results of many classifications confirm this finding.

Conversely, a binary mask was also created to eliminate water bodies. This was important in this region of interest because after applying the panchromatic band sharpening, all of the water body pixels were eliminated in the post-event imagery, but many of the pixels retained small values in some bands in the pre-event imagery. By creating a binary mask with values of zero where all bands in a pixel had values below 12, the mask was applied to successfully eliminate all water bodies during classification which eliminated any chance of poor results due to water body anomalies.

Successful classification of land use at a low resolution is important for remote sensing because this data is freely available and exists for all areas of the world at many different time periods. Furthermore, concluding which classification method is preferred is important to quickly and accurately classify images when panchromatic bands are available, which is the case for most Landsat 7 level 1 images. Pixel counts for 9 classes in the maximum likelihood classification of the multispectral bands is shown in **table 1.** The purpose of this project is to estimate types and quantities of infrastructure which exist in vulnerable areas due to earthquake risks, but similar methodologies can be applies for risks due to any other natural hazards in other areas of the world. Linking the value of losses seen in this earthquake in each class with the number of pixels in each class produces a dollar value of loss per pixel (**table 2)**. Ultimately, this methodology reduces our reliance on GIS maps to accurately portray infrastructure layers in areas of interest by directly analyzing the infrastructure locations through remote sensing techniques.

Table 1: Pixel count and percent per class in maximum likelihood classification on original image with no threshold and water body mask applied.

Class Summary	Pixel Count	Percent
Unclassified	39971	9.00
Roads	60835	13.70
Port	842	0.19
Buildings	5075	1.14
Fields	40581	9.14
Parking	5876	1.32
WideFlatBuildings	18367	4.14
Residential	63934	14.40
Woods	177633	40.00
Highways	30966	6.97

Table 2: Damage per **road** pixel found by maximum likelihood classification method.

Recorded Damage (2018 USD)	Number of Pixels	Damage per Pixel
$3,443,037.50	60,835	56.6

This project also highlights the need for higher resolution data. As discussed earlier, images at 30-meter resolution did not reveal much change detection or enough detail to successfully differentiate features such as roads versus trees that line the roads. As discovered in this project, after much trial and error, 15-meter resolution was found to successfully classify some areas in conjunction with a binary mask to eliminate water bodies but change detection at the same resolution was only mildly successful. As many of the features we are looking at for classification, such as roads and trees, are smaller than 15 meters, it stands to reason that higher resolution data could help to more successfully classify these areas. Similarly, if damage to a road or building is less than 15 meters across, then higher resolution pixels could help to more successfully constrain the damage seen.

Completeness & Future Work

This project was completed utilizing many of the tools learned during the course, "*UEP-0189*", such as filters, indices, binary masks, color slicing, band math, panchromatic band sharpening, and several classification methods. However, due to the only moderate results achieved, the project could likely be improved by using more sophisticated techniques not yet addressed in the course, such as a neural network for classification. A neural network technique will likely require higher spatial resolution data, larger quantities of training pixels, and more computing power, all of which were not able to be obtained for a short-term class project.

There are also likely some complex indices or textural filters or outside of the scope of this course which would have improved results using the change detection and classification methods learned in the course. As some meaningful results within were achieved within the bounds of the project, these more complex techniques were not necessary, though in future work they could add value to classification and change detection.

Another way the change detection results could have been improved was to increase the temporal resolution in regard to the earthquake itself. As mentioned earlier, the pre-event image was taken three weeks before the event and the post-event image was taken three weeks after the event. The change in seasonality alone likely changed some of the values, thus distorting change results, as the sun's elevation angle was changed in addition to increasing vegetation. Applying some more complex corrections to account for these differences would have been difficult but may have slightly increased results. Alternately, by increasing the temporal resolution, by obtaining pre- and post-event imagery only three days away from the event instead of three weeks, these errors would have been minimized and the complex corrections would likely be unnecessary.

Overall, most of the project was completed as planned, with additional focus placed on the classification improvements instead of change detection, especially at 30-meter resolution, which showed much less potential for success.

References

1. Nisqually Geotechnical Extreme Events Reconnaissance (GEER) Association. (2001). Retrieved April 2020, from http://geerassociation.org/
2. USGS. (2001). Home. Retrieved April 2020, from https://earthexplorer.usgs.gov/
3. Laben, Craig A., and Bernard V. Brower. Process for Enhancing the Spatial Resolution of Multispectral Imagery using Pan-Sharpening. US Patent 6,011,875, filed April 29, 1998, and issued January 4, 2000.
4. Zha, Y., J. Gao, and S. Ni. "Use of Normalized Difference Built-Up Index in Automatically Mapping Urban Areas from TM Imagery." *International Journal of Remote Sensing* 24, no. 3 (2003): 583-594.
5. Mather, P. M., & Koch, M. (2011). *Computer processing of remotely-sensed images: an introduction*. Hoboken, N.J: Wiley-Blackwell. Chapters 6 and 8.